Mine Water and the Environment (2021) 40:345–356
https://doi.org/10.1007/s10230-021-00765-3

TECHNICAL ARTICLE

Prevention and Control of Water Inrushes from Subseam Karstic Ordovician Limestone During Coal Mining Above Ultra-thin Aquitards

Xiaolong Li[1,2,3] · Shuning Dong[2,3] · Kaide Liu[4]

Received: 8 April 2020 / Accepted: 1 March 2021 / Published online: 11 March 2021

Abstract
Horizontal directional drilling technology was used to prevent and control water inrushes from the Ordovician limestone strata at the Sangshuping coal mine in the Hancheng mining area by drilling and grouting the contact zone along the top of the aquifer. Considering the hydraulic conductivity of the floor failure zone, we used the modified water inrush coefficient method to estimate the critical thickness of Ordovician limestone that had to be grouted. We carried out directional borehole exploration from both ends of the mining face and combined the results with borehole water pressure tests to determine appropriate grouting techniques and parameters; we then analysed the effectiveness of the grouting. 3-D seismic and ground transient electromagnetics (TEM) were used to detect areas of anomalous resistivity and geologic structure in the mining area, while DC and TEM geophysics were used to detect water-bearing areas ahead of the roadway. After the roadway was developed, TEM, DC resistivity sounding, and audio-magnetotellurics were used to explore water-bearing areas under the roadway and the mine floor. Radio waves were used to detect the structure of the mining face and changes in coal thickness. Finally, based on the results of exploration, an inspection program was devised using conventional boreholes supplemented by directional boreholes to comprehensively evaluate the feasibility of mining under pressure. The study showed that the failure depth of the floor was 15 m and that the top of the Ordovician limestone was no longer water-bearing and was now a relative aquitard. The water inrush coefficient was reduced to less than 0.073 MPa/m, which will ensure safe mining and extend the lower limit of safe mining in the area. This provides a technical reference for prevention and control of Ordovician limestone water disasters in similar coal mines.

Keywords China · Directional borehole · Grouting · Hydrogeological condition · Water inrush coefficient · Transient electromagnetics

Introduction

During the period of 2011 to 2015, 17 serious water inrush accidents occurred in China's coal mines, causing 229 deaths. Water inrushes associated with Ordovician limestone below the floor is an important issue restricting the safe mining of Permian-Carboniferous-age, Huabei-type coalfields in China. With increasing production levels and depths of coal mining, the higher hydrostatic pressures create serious water inrush problems (Wu et al. 2006).

Since the early 2000s, researchers have proposed various ways to evaluate the problem of water inrushes into coal mine workings from confined aquifers lying short distances below (Dong et al. 2020; Hu et al. 2019; Li 2018; Li et al. 2018a, b; Liu et al. 2018; Qiu et al. 2017; Wu et al. 2011, 2013, 2016, 2017; Yang et al. 2017; Yin et al. 2016). These evaluation methods range from the water inrush coefficient (or modifications to it) to physical and numerical models. Proposed treatment methods include reinforcement by grouting of the coal seam itself, the strata below the coal seam and combinations of both. Conventional borehole grouting has been used to cement off water inrushes in the deeper coal

✉ Xiaolong Li
Lxlxust@163.com

1 College of Geology and Environment, Xi'an University of Science and Technology, Xi'an 710054, China

2 Xi'an Research Institute, China Coal Technology and Engineering Group Corp., Xi'an 710077, China

3 Shaanxi Key Laboratory of Preventing and Controlling Coal Mine Water Hazard, Xi'an, 710077, China, Xi'an 710077, China

4 Shaanxi Key Laboratory of Safety and Durability of Concrete Structure, Xijing University, Xi'an 710123, Shaanxi, China

seams of the Weibei coalfield during mining. To ensure that grouting is effective, it is imperative to be able to accurately estimate the critical thickness for a reinforced aquitard in the floor prior to starting a grouting program. It is also necessary to minimize the cost of water inrush control and develop a consistent procedure for preventing and controlling water inrushes from the Ordovician limestone.

There has been much research on prevention and control of water inrushes from the Ordovician limestone, but much of it has involved prediction methods rather than inrush control (Dai et al. 2018). Since 2013, near-horizontal directional drilling technology has been used to prevent and control water inrushes from the Ordovician limestone. This article focuses on the prevention and control of water inrush at mining faces 3105, 3104, 3110, and 3109 of the no. 11 coal seam in the Sangshuping coal mine (Fig. 1), where the strata immediately below the seam is characterized by extremely thin aquitards lying above Ordovician limestone aquifers. The limited thickness of the aquitard is insufficient to restrain the pressurized water, which results in inrush accidents.

Background

General Situation

The Sangshuping coal mine is located in the northernmost west bank of the Yellow River in the Hancheng mining area of the Weibei coalfield. Coal seams no. 3 and no. 11 are the main ones being mined. The no. 3 seam is subject to gas outbursts, while the no. 11 seam is a deeper seam that protects the no. 3 seam. The no. 11 seam in the Nanyi mining area is 15–33 m above the upper contact of the Ordovician limestone strata. The static (artesian) water level elevation of the Ordovician limestone is + 375 m, while the elevation of the no. 11 coal seam is below + 375 m. The integrity of the coal seam floor is poor, the water-bearing nature of the Ordovician limestone aquifer is uneven, and there is a high risk of water inrushes from the Ordovician limestone. The isopach of the thickness of the interface between the floor of no. 11 coal seam and the upper contact of the Ordovician limestone is shown in Fig. 1; the location of the Sangshuping coal mine is shown in Fig. 2.

Geological Conditions

The no. 11 coal seam is located in the lower part of Taiyuan formation of the Upper Carboniferous. The mining field is located in the eastern part of the Weibei uplift on the southeastern margin of the Ordos block. The basic shape is a monocline structure, the formation dip angle is about 8°, and there are no important faults.

Hydrogeological Conditions

The uppermost aquifer is a phreatic porous aquifer group of a Quaternary sand and gravel layer. Below this are a confined fractured Permian sandstone aquifer of low permeability, a confined fractured Carboniferous sandstone or limestone aquifer of low permeability, and a confined Ordovician

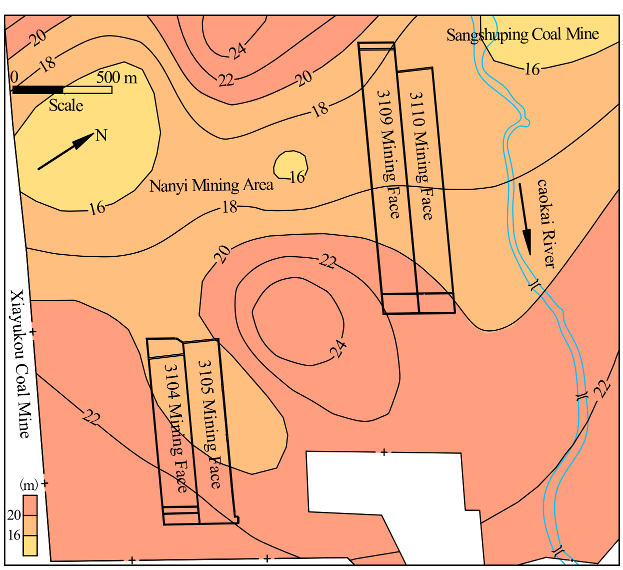

Fig. 1 The isopach of the thickness of the interface between the floor of the no. 11 coal seam and the upper contact of the Ordovician limestone

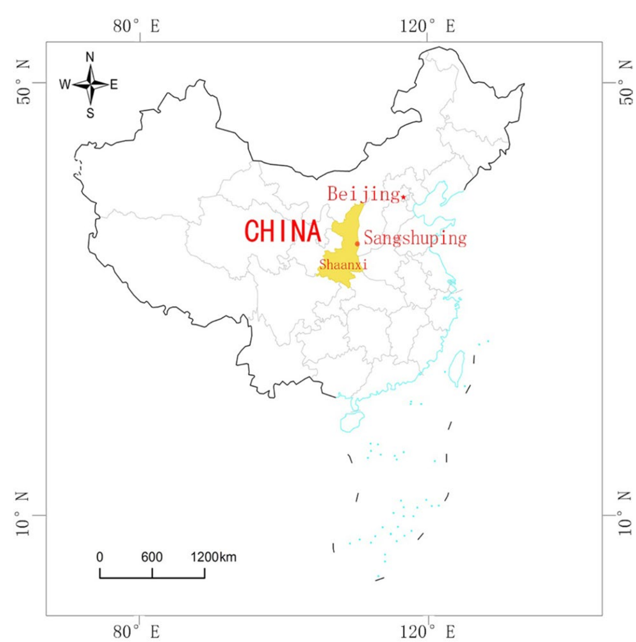

Fig. 2 Location of the Sangshuping coal mine

limestone karst aquifer group with alternating fracture and karst channel porosity. The segment of the Fengfeng Formation at the top of the Ordovician limestone was water-bearing, while just below it was a relative aquitard. The upper segment is directly connected to the coal measure strata and lies very close to the no. 11 coal seam, making it a direct threat to safe mining. The relative positions of the no. 11 seam, the aquifers, and aquitards are shown in Fig. 3.

The main aquitards that play a protective role in the mining of the no. 11 coal seam are Carboniferous mudstone, siltstone, and the basal weathered filling zone with relatively low hydraulic conductivity on top of the Ordovician limestone (Wang et al. 2019).

Since the establishment of the coal mine, there have been nine water inrushes, mainly from the upper segment of the Fengfeng Formation. The most serious incident, which halted production, was in August 2011; the water inrush discharge averaged 6,580 m^3/h and peaked at 13,200 m^3/h.

Prevention and Control of Inrushes from the Ordovician limestone

This paper addresses the use of near-horizontal directional boreholes to grout the upper contact of the Ordovician limestone below the floor. The directional borehole pattern for grouting this zone is shown in Fig. 4.

Design of grouting for control of water inrushes during roadway excavation and mining requires definition of the required aquitard thickness above the Ordovician limestone aquifer.

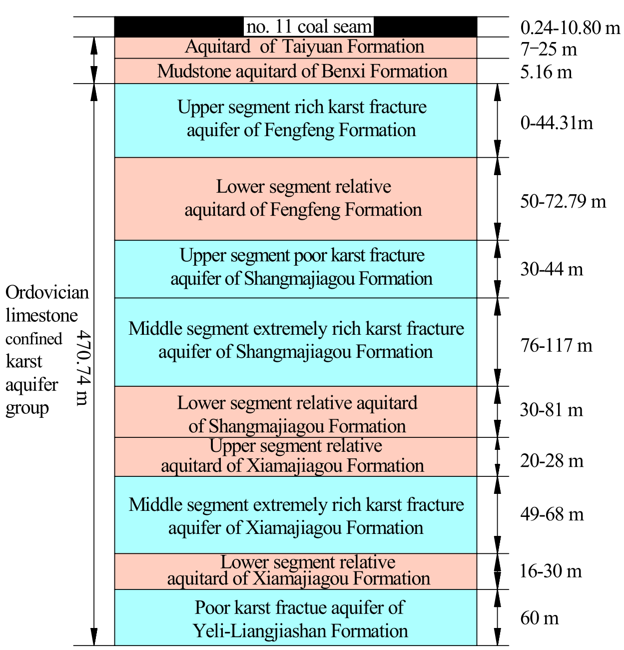

Fig. 3 Relative positions of the no. 11 coal seam, aquifers, and aquitards

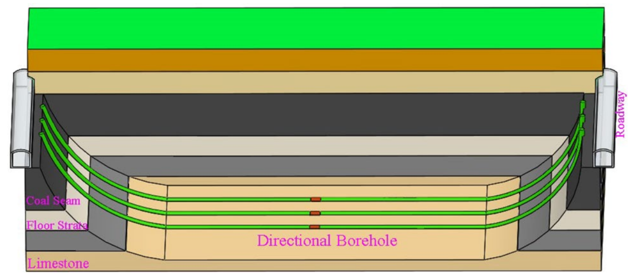

Fig. 4 The directional borehole pattern for grouting

Prevention and Control of Inrushes for Roadway Excavation

First, directional boreholes were used to explore the target strata at the upper contact of the Ordovician limestone. Structurally anomalous and water-bearing areas were reinforced by grouting. If no anomalous area was found from borehole exploration, then transient electromagnetic (TEM) or direct current (DC) methods was used to detect low-resistivity anomalies directly in front of the roadway (and up to 80 m below). Anomalous areas were checked by conventional and directional boreholes. Finally, the effectiveness of the preventive and control measures was evaluated by the presence or absence of seeps.

Prevention and Control of Inrushes for Mining

First, directional boreholes were used to fully explore the strata between the roadway and the upper contact of the Ordovician limestone. Structurally anomalous and water-bearing areas were remediated by grouting. Second, after development of the roadway system, audio-magnetotellurics (AMT) was used in the roadway to detect water-bearing anomalous area below the floor of the mining face (0–60 m depth), and the radio wave perspective technique was used to detect the internal structure of the coal seam and changes in coal thickness. Third, after combining the results of the directional borehole and geophysical exploration, anomalous areas were checked by conventional and directional boreholes. Finally, the effectiveness of all of these measures was evaluated. After all anomalies were addressed, mining could start.

Study of the Fractured Depth of the Coal Seam Floor

The key to successful prevention and control of water inrushes was the use of directional borehole for exploration and grouting reinforcement of the top of the Ordovician limestone strata. The selection of the thickness of strata to reinforce by grouting was very important, since floor stress is redistributed by the process of mining. Based on the concept of the "three zones under coal seams", we anticipated a fractured zone in the immediate floor due to stress redistribution followed by a relatively impermeable zone, and then the water-bearing Ordovician limestone. The fractured zone could not be allowed to extend to and connect with the confined aquifer.

Estimation of the Fractured Depth in the Floor

The Sangshuping coal mine uses longwall mining; a 2 m wide concrete wall was constructed inside the tracked roadway as mining proceeded. The maximum fractured depth in the floor was generally located in the goaf behind the coal wall (Zhang et al. 1990). To define the fractured depth in mining face 3105, four boreholes (TC1, TC2, TC3, and TC4) were drilled in the tracked roadway. Borehole water pressure and sound wave travel-time tests as well as borehole cameras were used to comprehensively observe and study the fracture depth. The testing intervals for the three tests were 50 m before mining and 60 m after mining. A borehole plan and profile are shown in Fig. 5. The borehole information for the tests is shown in Table 1.

Borehole Water Pressure Test

The main purpose of the water pressure test was to measure the permeability of the rock mass. The depth of mining-related fractures in the floor was estimated by comparing the change in the hydraulic conductivity of the floor before and after mining. The original hydraulic conductivity was k_1, the hydraulic conductivity after mining was k_2, which is related to k_1; ΔK was the increase in permeability (K_2—K_1) and K_2/K_1 was the permeability ratio. First, a double packer device was used to inject water into discrete length intervals to determine K_1. The volume of water injected into the four boreholes was very small, so K_1 was determined from single packer tests. The test pressure was 0.2 MPa, the water pressurization time was 15–25 min, and pressure data were recorded every 5 min. In the 8–10 m test section of borehole TC1, the volume of water injected increased with a single packer, and blocks fell out into the borehole, showing that this section was within the fractured zone; thus, an initial undisturbed hydraulic conductivity could not be obtained. Variations in water injection volume with mining distance is shown in Fig. 6. The hydraulic conductivity calculation of each test section is shown in Table 2.

The premining hydraulic conductivity of borehole TC2, as measured by a single packer water pressure test, was 0.09 m/d. A large volume of water was required for the single packer water pressure test, so a double packer

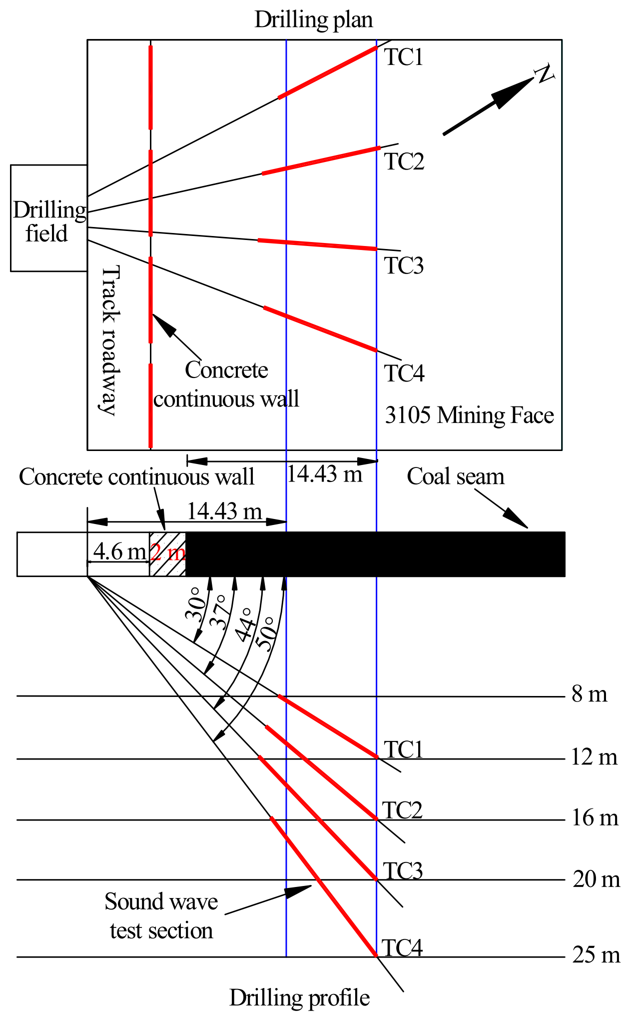

Fig. 5 Borehole plan and profile

Table 1 Borehole information for the testing of floor fractured depth

Borehole	Azimuth angle (°)	Inclination angle (°)	Depth (m)	Range of the vertical test section (m)
TC1	354	30	29	8–12
TC2	8	37	29	10–16
TC3	28	44	32	12–20
TC4	42	50	37	16–25

was used to inject the water in discrete length intervals. The test sections were at 10.1–10.3 m, 11.1–11.3 m, 12.0–12.2 m, 12.9–13.1 m, 13.8–14.0 m, 14.7–14.9 m, and 15.6–15.8 m. As can be seen in Fig. 6, the vertical depth was 10.1–14.9 m and the volume of water fluctuated greatly. The maximum flow values of 6–12 L/min were found about 5–10 m after the mining face had passed the measuring point. This shows that the development of rock mass fractures in different sections differed due to

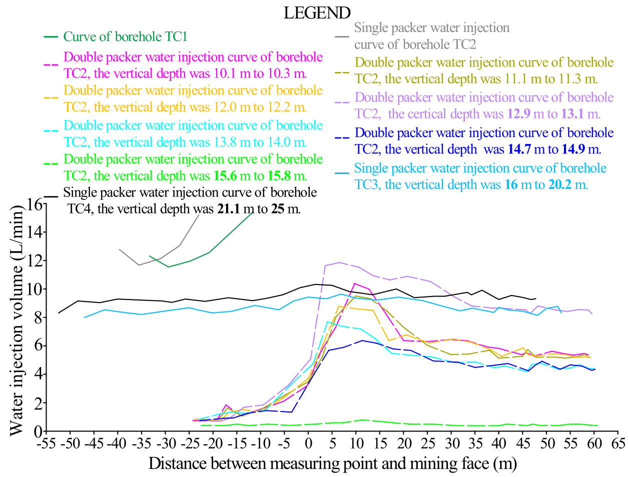

Fig. 6 Variations in water injection volume with mining distance

Table 2 Calculation of the hydraulic conductivity of each test section

Borehole	Test depth (m)	K_1 (m/d)	K_2 (m/d)	K_2/K_1	ΔK (m/d)
TC 2	10.1–10.3	0.09	2.21	23.49	2.11
	11.1–11.3	0.09	2.03	21.66	1.94
	12.0–12.2	0.09	1.86	19.84	1.77
	12.9–13.1	0.09	2.50	26.68	2.41
	13.8–14.0	0.09	1.63	17.33	1.53
	14.7–14.9	0.09	1.35	14.37	1.26
	15.6–15.8	0.09	0.17	2.3	0.08
TC 3	16.0–20.2	0.06	0.07	1.1	0.01
TC 4	21.1–25.0	0.06	0.08	1.2	0.02

the influence of mining. The volume of water injected into the section from 15.6 to 15.8 m was basically unchanged across the full length of the test, which showed that mining had little influence on this section.

The premining hydraulic conductivity of boreholes TC3 and TC4 was 0.06 m/d. The test sections in boreholes TC3 and TC4 were located at 16–20.2 m and 21.1–25.0 m, respectively. Figure 6 shows that there was almost no change in the volume of water injected into the test section from the beginning to the end. The curve was relatively stable, indicating that mining had almost no effect on these sections.

Table 2 shows that the premining and postmining hydraulic conductivity in the test section at 10.1–14.9 m in borehole TC2 satisfied the permeability index criteria $\Delta K \geq 0.2$ and $K_2/K_1 \geq 2$ (Zhang et al. 2016), indicating that this depth was within a fractured zone. The change in hydraulic conductivity in each test section of the other boreholes did not meet this requirement. Therefore, the disturbance failure depth of the floor measured by the water pressure test was 14.9 m.

Sound Wave Travel Time Tests

Sound waves travel times in a rock mass can also be used to detect stress changes and floor fractured depth in a mining face. During the mining period, a data monitoring line was arranged in each of the four boreholes in mining face 3105 with CLC1000 ultrasonic surrounding rock fracture detectors (Wang 2020). The effective vertical observation depth was 10–25 m. The tests began when the distance from the mining face to the test borehole was about -36 m and finished at about 56.7 m after mining. The observation positions were at −36 m, −23 m, −14 m, −1.1 m, 6 m, 18 m, 34 m, and 56.7 m. The "time-high" curve verified that the stress at any point in the floor strata during mining and the resultant displacement of the coal seam floor had three stages: premining rise, postmining decrease, and recovery. The sound wave travel time curves at different distances from the borehole to the mining face are shown in Fig. 7.

From −36 m to −14 m, the coal seam floor went from the original stress state to the initial disturbance stage. The "time-high" curve was at a low magnitude, reflecting a rapid wave velocity, and the curve was relatively stable.

From −14 to 34 m, at a fixed observation position, the "time-high" curve obviously changed from high to low, indicating that the wave velocity increased greatly. With increasing vertical depth, the rock mass of the coal seam floor changed from broken to complete, with the broken area occurring at depths of 10–14.7 m. The "time-high" curve of the test section from 14.7 to 25 m was in a low and stable stage, and the coal seam floor was still in the elastic region. It can be seen that coal seam floor fractures had not developed to this depth.

From 34 to 56.7 m, the "time-high" curve was in a low and stable stage, indicating that the wave velocity was fast. The rock mass with plastic failure in the shallow part of the coal seam floor was gradually closed, and the roof was recompacted, but the fracturing phenomenon did not occur again.

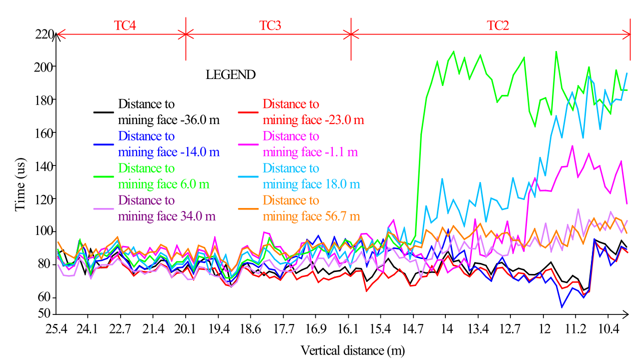

Fig. 7 The sound wave travel time curves at different distances from the borehole to the mining face

Borehole Camera Surveys

Broken, vertical, and transverse fractures in the floor rock mass were observed using a YSZ (B) type borehole camera. There were many fractures developed at 10–15 m, but no fractures were observed below 15 m, and the rock mass was relatively complete. Considering the three field measurement methods comprehensively, it was considered that the fractured floor depth was 15 m, which accords with the real situation.

Analysis of the Fractured Floor Depth at the Other Mining Faces

The fractured floor depth was found to be proportional to the mining depth, mining width and mining height, and related to the mechanical properties of the rock mass and the angle of the coal seam; mining depth and mining face size had the greatest influence. Mining faces 3104, 3110, 3109, and 3105 were in the same mining area and the mining face size, angle, and lithologies of roof and floor were the same. Therefore, it was judged feasible to calculate the fractured floor depth in the Nanyi mining area using the measured depth at mining face 3105.

Directional Borehole Exploration and Grouting Reinforcement of the Ordovician Limestone

From the above study, it can be seen that safe entry development and mining required that the top of the water-bearing Ordovician limestone had to be maintained at a satisfactory distance below the fractured subseam zone, considering the loss of water resistance in the fractured zone and using the upper limit of the coefficient stipulated in *The Detailed Rules for Water Disaster Prevention and Control of Coal Mines* (NCMSA 2018). The lower limit of the critical aquitard thickness was calculated to determine the critical thickness necessary for the grouting reinforcement. The water-content within the critical aquitard zone above the upper contact of the Ordovician limestone was explored by directional boreholes. As already mentioned, the upper segment of the Fengfeng Formation at the top of the Ordovician limestone was water-bearing, with a relative aquitard below it. Because the upper segment was not a traditional aquifer, the directional boreholes had to traverse the full thickness of the aquifer to comprehensively explore its water-bearing nature. If this segment was thick enough, then it could be grouted to transform it into an aquitard with sufficient impermeability and thickness to ensure safe mining.

Critical Formation Selection for Exploration and Grouting Reinforcement

Formula Derivation for Calculating the Critical Thickness of a Grouted Aquitard

The water inrush coefficient (WIC) formula found in Appendix 5 of *The Detailed Rules for Water Disaster Prevention and Control of Coal Mines* (NCMSA 2018) states that the water inrush coefficient should not exceed 0.06 MPa/m in an area where the coal seam floor has been fractured or 0.1 MPa/m in an unfractured area. The water inrush coefficient formula is:

$$T = \frac{P}{M} \tag{1}$$

where T is the water inrush coefficient (MPa/m), P is the actual water pressure at the base of the floor aquitard (MPa), and M is the thickness of the aquitard below the floor (m). The water pressure should be determined at the top interface of the aquifer based on the highest water level observed in the aquifer duering the past three years. The P_2 at the base of the aquitard after exploration and grouting is:

$$P_2 = \frac{h - H + M_d + M_c}{100} \tag{2}$$

where H is the elevation of the coal seam floor (m), h is the water level of Ordovician limestone (+375 m), M_c is the critical thickness on top of Ordovician limestone (m), and M_d is the fractured depth of the floor (15 m). The term h and H were absolute value. After exploration and grouting, Eq. (1) is given by:

$$T_2 = \frac{P_2}{M_c} \tag{3}$$

where T_2 is the required water inrush coefficient after grouting (0.06 MPa/m). Combining Eqs. (2) and (3) and rearranging, the critical aquitard thickness Mc is given by:

$$M_c = \frac{h - H + M_d}{100T_2 - 1} \tag{4}$$

The critical aquitard thickness formula obtained was reliable, and the results were therefore used to determine the critical thickness at the upper contact of Ordovician limestone of exploration and grouting reinforcement.

Isopach of the Grouted Aquitard Above the top of the Ordovician Limestone Aquifer

Based on data from 193 boreholes in the mining field, the critical thickness of the grouted aquitard at each borehole was calculated by Formula (4). The isopach of the fractured depth plus grouted aquitard thicknesses based on a fractured zone depth of 15 m is shown in Fig. 8. From the isopach map, it can be seen that the critical thickness of the grouted aquitard in mining faces 3105 and 3104 gradually deepened from the terminal line to the initial cut off the set-up entry; it was located 28–44 m below the coal seam floor (an average of 34 m). The critical thickness of the grouted aquitard in mining faces 3110 and 3109 gradually deepened from the terminal line to the initial cut off the set-up entry; it was located 48–61 m below the coal seam floor (an average of 54 m).

Exploration Procedure for Grouting

Based on Fig. 8, 45 near-horizontal directional boreholes were advanced between the top of the water-bearing Ordovician limestone and the fractured zone below the coal seam. The azimuth of the boreholes was the same as the strike of the mining face. The initial dip angle of the boreholes was the maximum angle of the drilling rig (−20°), to reach the design depth as soon as possible; then the dip angle was increased to drill steadily along the design stratum. The horizontal section of the directional borehole was 40 m wide and the width of the mining face was 180 m. Each mining face was arranged with 4–6 pairs of directional boreholes to achieve full-coverage, with a mining length of 1200 m and an average borehole length of 650 m.

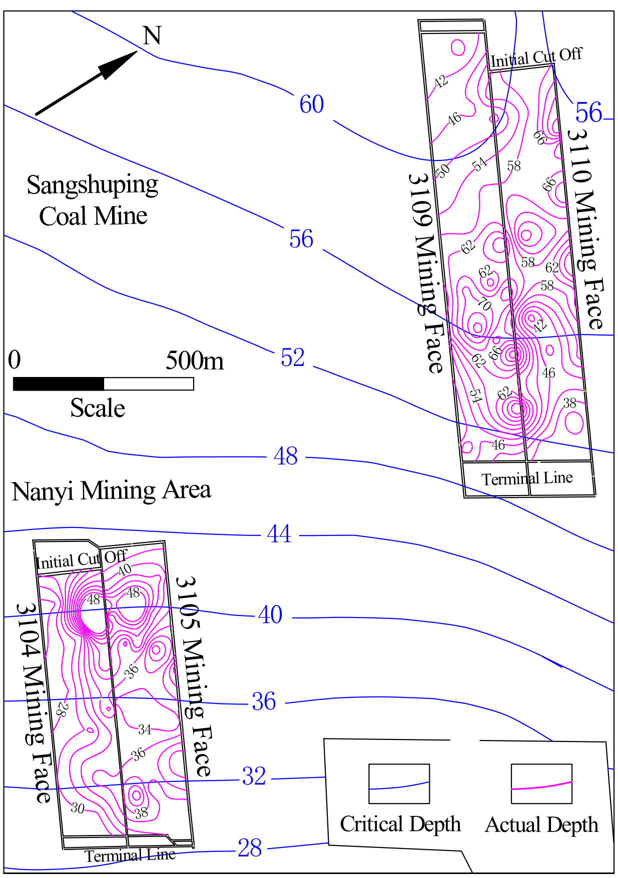

Fig. 8 The isopach of the relationship between the critical depth and actual exploration depth

Twelve directional boreholes were constructed in mining face 3105. Among them, three boreholes had water outflow. The rate of water outflow was 2.1–5 m^3/h and the maximum water pressure was 0.12 MPa. The exploration depth was 28–59 m below the coal seam floor (an average of 40 m), exceeding the critical average depth of 34 m. The depth to which the Ordovician limestone was explored was 10–39 m (an average of 20 m).

Eight directional boreholes were constructed in mining face 3104. Among them, four boreholes had water outflow; the rate of water outflow was 0–5.4 m^3/h, and the maximum water pressure was 0.15 MPa. The actual exploration depth was 27–77 m below the coal seam floor (an average of 36 m), exceeding the critical average depth of 34 m. The depth to which the Ordovician limestone was explored was 6–58 m (an average of 15 m).

Thirteen directional boreholes were constructed in mining face 3110. Among them, two boreholes had water outflows of 0.1–0.22 m^3/h. The actual exploration depth was located 31–82 m below the coal seam floor with an average of 54 m, which was consistent with the critical average depth. The depth to which Ordovician limestone was explored was 11–65 m (an average of 35 m).

Twelve directional boreholes were constructed in mining face 3109. Among them, three boreholes had water outflow. The rate of water outflow was 0.12–1.34 m^3/h. The actual exploration section was located 37–83 m below the coal seam floor (an average of 56 m), which exceeded the critical average depth of 54 m. The depth to which the Ordovician limestone was explored was 17–64 m, with an average of 37 m.

An isopach map of floor exploration and grouting reinforcement was drawn based on the actual exploration depth of the directional boreholes (Fig. 8, Table S-1). The relationship between the critical depth and actual exploration depth was analysed. The latter was generally consistent with the coal seam floor, with a strike of 114°/294° and dip to 24°. Directional boreholes formed an exploration plane to cover each mining face. The average exploration thickness of faces 3105, 3104, and 3109 all exceeded the critical thickness. The average exploration thickness of mining face 3110 was equal to the critical thickness. The actual planar trajectory is shown in Fig. 9.

Grouting Reinforcement of the Ordovician Limestone

The Ordovician limestone was reinforced by grouting, based on the exploration results of the directional borehole. The grouting parameters were determined based on water pressure tests carried out to define the formation water permeability.

Water Pressure Tests

In situ water pressure test data were used to calculate the permeability to truly reflect the geological conditions and rock mass structure. The formula we used was based on a conventional vertical borehole water pressure test, which can also be used to calculate permeability in near-horizontal sections of directional boreholes, as it reflects the average permeability in the test section, per the Lugeon test calculation model (Vaskou et al. 2019). So rapid water injection from the orifice to the borehole was used, which was similar to a single packer water pressure test.

The water injection pressure is the sum of the orifice pressure and static water pressure of the water column in the borehole. A borehole high-pressure water pressure test should not be conducted at less than 1.2 times the hydrostatic pressure. The elevation of mining faces 3110 and 3109 was 100 m lower than that of 3105 and 3104, so it was necessary to set P_0 accordingly. We calculated the water injection pressure according to Formula (5).

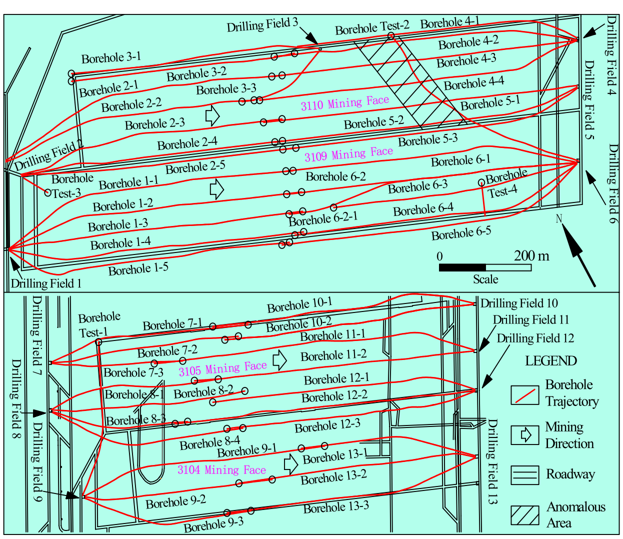

Fig. 9 Actual plane trajectory

$$P_0 = P_m + \frac{H - h}{100} \tag{5}$$

where P_0 is the water injection pressure (MPa), P_m is the orifice pressure (MPa), H is the vertical distance from the orifice to the midsection of the injected formation (m), and h is the height of the water column at the midpoint of the injected formation before water injection (m).

The average water pressure of the Ordovician limestone in the exploration strata at mining faces 3110 and 3109 was 2.5 MPa, P_0 was 3 MPa, H was 28 m, and h was 224 m. Without considering the pressure loss, $P_m = 5$ MPa, so three levels of pressure and five test stages were adopted in the order of $1 \rightarrow 3 \rightarrow 5 \rightarrow 3 \rightarrow 1$ MPa to obtain the permeability in situ.

For mining faces 3105 and 3104, The average water pressure was 1.3 MPa, P_0 was 1.6 MPa, H was 30 m, and h was 100 m. Without considering the pressure loss, $P_m = 2.3$ MPa was obtained, so three levels of pressure and five test stages were adopted in the order of $1 \rightarrow 2 \rightarrow 3 \rightarrow 2 \rightarrow 1$ MPa to obtain the permeability in situ.

It can be seen from supplemental Table S-1 that only boreholes 1–3 and 9–2 had hydraulic conductivities exceeding 10^{-6} cm/s. Among the rest, the hydraulic conductivity of borehole 1–3 was 3.3×10^{-6} cm/s, which was very low. The hydraulic conductivity of borehole 9–2 was 8.5×10^{-6} cm/s, because the borehole drilled into the fractured sandstone strata. Comparing the calculations of permeability with the *Rock Permeability Classification Table* (Yang et al. 2018), it can be seen that the upper segment of the Fengfeng Formation is now micro-permeable. The fracture connectivity was not developed, so it can be regarded as a relative aquitard.

Grouting Technology and Parameters

The Ordovician limestone contains blind fissures, network-like open fissures, karst caves, and other void spaces. In this application, borehole bottom grouting and orifice grouting were used. To plug the cracks more fully, a sectional downward grouting method was adopted, which combines continuous and intermittent grouting. When the rate of water outflow from the borehole was less than 50 m^3/h, grouting was started every 100 m. If the rate of water outflow was more than 50 m^3/h, or if a karst cave was encountered, the drilling was stopped, and grouting was started.

Analysis of Grouting Effects

According to the exploration results, boreholes 8–1, 8–2, 8–3, 8–4, 9–1, 9–2, and 9–3 all had water outflow rates between 2.1–5.4 m^3/h (Table S-1). The orifice positions of these seven boreholes were all located in the sandstone formation immediately upper the coal seam. The water pressure was much less than normal Ordovician limestone water pressure. A large amount of H_2S gas was carried in the water in the sandstone fractures. Therefore, sandstone formation grouting was carried out.

In boreholes 1–5, 2–5, 4–1, and 5–3, water outflow occurred when drilling into the Ordovician limestone (Table S-1). The rates of water outflow ranged from 0.12 to 1.34 m^3/h, and there were no cases where the instantaneous rate of water outflow exceeded 50 m^3/h. The rest of the boreholes did not produce water. This shows that the fracture connectivity of the Ordovician limestone formation was poor. Only borehole sealing was required and it was carried out using a grouting pressure of 5 MPa.

Post-Grouting Geophysical Exploration and Inspection using Borings

3-D seismic and ground TEM were conducted in the Nanyi mining area to examine the hydrogeological conditions of the Ordovician limestone aquifers and effectively reduce the occurrence of water inrush accidents. After completion of directional borehole exploration and grouting reinforcement, DC (Li et al. 2015; Xue et al. 2019) or a TEM method (Xue et al. 2019) was used underground to detect low-resistivity anomalous areas in front of the roadway. The roadway excavation lengths were determined from the geophysical results, until the roadway system was formed. TEM sounding or DC resistivity sounding was performed to depths of 80 m, AMT was performed to 30 and 60 m depths, and radio wave evaluation was also carried out. In addition, anomalous areas were checked by conventional and directional boreholes.

Geophysical Exploration and Drilling Inspection Technology in Mining Face 3105

Mining face 3105 was the first to have grouting implemented. No low-resistivity anomalous areas were found by ground detection. Twenty-six DC and ten TEM advance explorations were carried out during roadway excavation. The single detection distance was 26–100 m, with a total of 33 anomalies. The overlapping anomalous area was mainly located in the initial cut off the set-up entry; the fractures (mostly roof fractures) were a result of the mining process.

TEM sounding, DC resistivity sounding, and AMT testing jointly detected a low-resistivity anomalous area at 20 m below the floor near the initial cut off the set-up entry. A special Test-1 directional borehole was aimed at the anomalous area (Fig. 9). When drilling to 129 m, the rate of water outflow was about 4.5 m^3/h and the water pressure was 0.19 MPa. The hydraulic conductivity was 1.78×10^{-6} cm/s. The rate of water outflow was small, and the water pressure was much less than the Ordovician limestone water pressure, indicating that this was a relatively closed stagnant area. No other anomalous structures and water-bearing areas were found.

Geophysical Exploration and Drilling Inspection Technology in Mining Face 3104

Mining face 3104, which shared the track roadway of mining face 3105, was the second to have grouting implemented. No low-resistivity anomalous area was found by ground detection. In the process of excavating the haulage roadway and the initial cut off the set-up entry, seven DC and three TEM advance detections were carried out at a detection distance of 80–100 m. Three anomalous areas were found, which were basically due to roof fractures or drastic changes of the coal seams. Actual excavation revealed no anomalous water-bearing areas.

DC resistivity sounding of the haulage roadway and AMT testing of the two roadways both found that there was an anomalous area in the initial cut off of the set-up entry. The coal seam was relatively broken by the process of excavating this initial cut off, so it was considered likely that the fractures under the floor were relatively developed. The exploration results of Test-1 found no anomalous structures or water-bearing areas. Similarly, no anomalous structure or water-bearing area were found in other anomalous areas.

Geophysical Exploration and Drilling Inspection Technology in Mining Face 3110

Mining face 3110 was the third to be grouted. A small fault was found in the track roadway by ground three-dimensional seismic exploration. When the track roadway was excavated here, a small fault was exposed. The ground TEM exploration showed that there were four low-resistivity areas, caused by the relative water-bearing nature of the roof sandstone; local dripping occurred from the roof during the roadway excavation. During this excavation, thirteen DC and three TEM explorations were carried out. The geophysical anomalous areas were exposed by excavation, and the only water that was found was dripping from the roof.

DC resistivity sounding found four, four, and one low-resistivity anomalous areas in the track roadway, haulage roadway, and initial cut off the set-up entry, respectively. Directional boreholes passed through all of these and no water-bearing areas were found.

Three low-resistivity anomalous areas respectively were found in the range of 0–30 m and 30–60 m below the floor by AMT at basically the same anomalous position. This was the reaction at different depths to the same anomalous area; again, no water-bearing area was found by directional drilling.

Radio wave perspective found two anomalous areas caused by faults and changes in coal thickness. Boreholes 4–1, 4–2, 4–4, 5–1, 5–2, and 5–3 had collapse and sticking phenomena. The geophysical data showed a wide range of obvious low-resistivity anomalous areas, suggesting a structural anomalous area in the upper part of the mining face (Fig. 9). The coal seam inclination angle changed greatly during the process of roadway excavation, making it impossible to drill in the Sect. 30–40 m below the floor. The borehole trajectory was adjusted to 41–82 m below the floor and no low-resistivity anomalous area was found during the drilling. To view the anomalous area, directional borehole Test-2 was designed (Fig. 9). It was drilled to 196.5 m, but the borehole could not pass through the collapsed area, so the direction was adjusted in the Sect. 50–65 m below the floor to pass through the area of collapse. No water was found and the water pressure test showed that the hydraulic conductivity was less than 10^{-6} cm/s.

Geophysical Exploration and Drilling Inspection Technology in Mining Face 3109

Mining face 3109, which shared the 3110 roadway, was the fourth to be grouted. Two small faults were found in the initial cut off the set-up entry and the return air roadway by three-dimensional seismic exploration. When the roadway was excavated here, there were no anomalous areas, and no water. Seventeen TEM advance detections were carried out during roadway excavation, and the length of single detection was 80–100 m. After all anomalous areas were excluded, the roadway was excavated for 60–70 m. The many anomalous areas were mainly due to roof fractures.

Three anomalous areas were detected by DC resistivity, AMT, and TEM sounding, and there were two anomalous areas in the haulage roadway and the initial cut off the set-up entry, which had water dripping from the roof during the excavation process. There was water seepage on the floor of another anomalous area in the haulage roadway, indicating that local fractures had developed.

The directional boreholes at the initial cut off the set-up entry were not completely covered, as again there was a sticking phenomenon in the Ordovician limestone during drilling. Two conventional inspection boreholes were specially designed on one side of the initial cut off the set-up entry and the mining face (Fig. 9). The designed depth of borehole Test-3 was 80 m and the final borehole depth was 80.5 m. After drilling to 56.5 m, water came from the borehole at a rate was less than 0.5 m^3/h. The designed depth of borehole Test-4 was 90 m. The final borehole depth was 60 m. When it was drilled to 37–43 m, there were sticking phenomena, but there was no water or leakage in the borehole. Water pressure testing showed that the hydraulic conductivity associated with the two boreholes was less than 10^{-6} cm/s.

Evaluation of Grouting Control for Prevention of Water Inrushes

Mining Under Pressure

Geophysical exploration and excavation revealed no large structures, and all low-resistivity anomalous areas were exposed. Exploration using boreholes showed that the top of Ordovician limestone was occasionally fractured but otherwise had very low permeability. The water pressure was much less than normal Ordovician limestone water pressure. There were no large karst fissures and the hydraulic conductivity was generally less than 10^{-6} cm/s. The explored thicknesses of the directional boreholes were greater than or equal to the critical thickness. It can be seen that the directional borehole exploration area of the upper segment of the Fengfeng Formation could indeed be used as a relative aquitard.

The water inrush coefficient after grouting was calculated based on the exploration thickness parameters. We compared the water inrush coefficient and the aquitard thickness before and after reinforcement by grouting. Considering the loss of water resistance capacity in the fractured zone of the immediate floor, the remaining thicknesses of the aquitard at mining faces 3105 and 3104 was 2–9 m before grouting; afterwards, they were 13.11–29.2 m and 11.2–62 m thick, respectively. The thickness increased by an average of 12 and 5.7 times, respectively. The average water inrush coefficient before the reinforcement was 0.33. After grouting, the average water inrush coefficients were 0.057 and 0.073, respectively, having decreased by 82.7% and 77.9%.

The effective thickness of the aquitard at mining faces 3110 and 3109 was 3–7 m before the reinforcement. Afterwards, the aquitard thicknesses were 16–67.1 m and 21.6–68.5 m, respectively; the thickness had been increased an average of 8.5 and 9 times, respectively. The average water inrush coefficient before grouting was 0.8; afterwards, they were 0.072 and 0.068, respectively, having decreased by 91% and 91.5%. To sum up, the reinforcement increased the thickness of the aquitard by 5.7–12 times and decreased the water inrush coefficient by 77.9%–91.5%, on average. The water inrush coefficients were all less than 0.1 MPa/m, which met the requirements of *The Detailed Rules for Water Disaster Prevention and Control of Coal Mines* (NCMSA 2018), so "mining under pressure" can be done. The aquitard thicknesses and water inrush coefficients before and after reinforcement of the mining face are shown in Table 3.

Table 3 The aquitard thicknesses and water inrush coefficients before and after reinforcement of the mining face

Mining face	Aquitard thickness (m)			Average water inrush coefficient (MPa/m)	
	Before reinforcement	Remaining	After reinforcement	Before reinforcement	After reinforcement
3105	17–24	2–9	13.11–29.2	0.33	0.057
3104	17–24	2–9	11.2–62	0.33	0.073
3110	17–22	3–7	16–67.1	0.8	0.072
3109	17–22	3–7	21.6–68.5	0.8	0.068

Water Flow through the Coal Seam Floor

A seepage of about 2 m^3/h was found in the haulage roadway floor of mining face 3105; it disappeared after two months. Similarly, there was about 2 m^3/h of seepage at the bottom of the coal wall in the roadway, 240 m from the initial cut off the set-up entry in face 3109. This rate of water outflow lasted for three months but didn't disappear; however, the rate of water no longer increased. In both cases, analysis demonstrated that the water had originated from the floor fracture zone. No water was found in the roadway of faces 3104 and 3110.

During mining, grouting was used in the goaf for the purpose of fire prevention. It was therefore difficult to judge whether the floor of the goaf was gushing water or not, but there were no obvious changes in the water sump, and it was judged that no delayed inrush had occurred in the goaf. All of the faces have since been mined safely, liberating 1.95 Mt of coal resources.

The safe mining outcome showed that in the Hancheng mining area, if the fractured zone's loss of water resistance capacity is considered, the modified water inrush coefficient method can be used to evaluate the feasibility of mining the no. 11 coal seam. The maximum water inrush coefficient can be selected as 0.073 MPa/m, which ensures safe mining. This provides a solid basis for further improving the critical value of the water inrush coefficient in *The Detailed Rules for Water Disaster Prevention and Control of Coal Mine* (NCMSA 2018).

Discussion and Conclusions

The upper portion of the Fengfeng Formation was converted by grouting into a thin aquitard with low permeability, a simple structure, low pore pressure, and undeveloped fractures. As a relative aquitard, it extended the lower limit of safe mining in Hancheng mining area. The three-field measurement method was used to determine that the floor failure depth of mining face 3105 was 15 m, which proved a suitable assumption for other mining faces in this coal field.

The water inrush coefficient was be reduced to less than 0.073 MPa/m after exploration and grouting. This provides a solid basis for further improving the determination of the critical value of water inrush coefficient in *The Detailed Rules for Water Disaster Prevention and Control of Coal Mine* (NCMSA 2018). It also provides guidance for mining under pressure in the Hancheng mining area.

Near-horizontal directional drilling technology in coal mines facilitates using a modified water inrush coefficient estimation method combined with an "exploration-grouting-inspection" approach to prevent and control water inrush. In the next research effort, the authors will study the diffusion radius of grouting in limestone strata as well as grouting process parameters. The spacing of directional boreholes will be optimised and procedures for preventing water inrushes from the Ordovician limestone will be improved.

Supplementary Information The online version contains supplementary material available at https://doi.org/10.1007/s10230-021-00765-3.

Acknowledgements This work was financially supported by the National Key R&D Program of China (Grant 2017YFC0804102), and the Shaanxi Key Laboratory of Preventing and Controlling Coal Mine Water Hazard. The authors express their sincere thanks to the reviewers for their valuable advice.

References

Dai GL, Xue XY, Xu K, Dong L, Niu C (2018) A GIS-based method of risk assessment on no. 11 coal-floor water inrush from Ordovician limestone in Hancheng mining area. China. Arab J Geosci 11:714

Dong SN, Zheng LW, Tang SL, Shi PZ (2020) A scientometric analysis of trends in coal mine water inrush prevention and control for the period 2000–2019. Mine Water Environ 39:3–12

Hu YB, Li WP, Wang QQ, Liu SL, Wang ZK (2019) Evaluation of water inrush risk from coal seam floors with an AHP–EWM algorithm and GIS. Environ Earth Sci 78(10):290

Li PY (2018) Mine water problems and solutions in China. Mine Water Environ 37:217–221

Li SC, Liu B, Nie LC, Liu ZY, Tian MZ, Wang SR, Su MX, Guo Q (2015) Detecting and monitoring of water inrush in tunnels and coal mines using direct current resistivity method: a review. J Rock Mech Geotech Eng 7(4):469–478

Li B, Wu Q, Duan XQ, Chen MY (2018a) risk analysis model of water inrush through the seam floor based on set pair analysis. Mine Water Environ 37:281–287

Li WP, Liu Y, Qiao W, Zhao CX, Yang DD, Guo QC (2018b) An improved vulnerability assessment model for floor water bursting from a confined aquifer based on the water inrush coefficient method. Mine Water Environ 37:196–204

Liu WT, Mu DR, Xie XX, Li Y, Wang DH (2018) Sensitivity analysis of the main factors controlling floor failure depth and a risk evaluation of floor water inrush for an inclined coal seam. Mine Water Environ 37:636–648

NCMSA (National Coal Mine Safety Administration) (2018) The Detailed Rules for Water Disaster Prevention and Control of Coal Mines. Coal Industry Publishing House of China, Beijing, pp 62–63 (in Chinese)

Qiu M, Shi LQ, Teng C, Zhou Y (2017) Assessment of water inrush risk using the fuzzy Delphi analytic hierarchy process and Grey relational analysis in the Liangzhuang Coal Mine, China. Mine Water Environ 36:39–50

Vaskou P, de Quadros EF, Kanji MA, Johnson T, Ekmekci M (2019) ISRM suggested method for the Lugeon test. Rock Mech Rock Eng 52:4155–4174

Water-resisting property and key technologies of grouting reconstruction of the Upper Ordovician limestone in north China's coalfields, Thesis, Xi'an Research Institute of China Coal Technology and Engineering Group Corporation https://doi.org/10.1007/978-3-030-40116-0

Wang QQ, Li WO, Liu QQ (2019) Geological composition and structure of the filling zone and its water-resisting property evaluation on top of the Ordovician limestone. Geofluids. https://doi.org/10.1155/2019/5140605

Wu Q, Wang MY (2006) Characterization of water bursting and discharge into underground mines with multi-layered ground-water flow systems in the north China coal basin. Hydrogeol J 14(6):882–893

Wu Q, Liu YZ, Yang L (2011) Using the vulnerable index method to assess the likelihood of a water inrush through the floor of a multi-seam coal mine in China. Mine Water Environ 30:54–60

Wu Q, Fan SK, Zhou WF, Liu SQ (2013) Application of the analytic hierarchy process to assessment of water inrush: a case study for the no. 11 coal seam in the Sanhejian Coal Mine. China. Mine Water Environ 32(3):229–238

Wu Q, Liu YZ, Wu XL, Liu SQ, Sun WJ, Zeng YF (2016) Assessment of groundwater inrush from underlying aquifers in Tunbai Coal Mine, Shanxi province, China. Environ Earth Sci 75(9):737

Wu Q, Guo XM, Shen JJ, Xu S, Liu SQ, Zeng YF (2017) Risk assessment of water inrush from aquifers underlying the Gushuyuan Coal Mine, China. Mine Water Environ 36:96–103

Xue GQ, Chen W, Cheng JL, Liu SC, Yu JC, Lei KX, Guo WB, Feng XH (2019) A review of electrical and electromagnetic methods for coal mine exploration in China. IEEE Access 7:177332–177341

Yang ZB, Dong SN (2018) Influence factors analysis of quantitative evaluation of single borehole grouting effect by water pressure test. Safe Coal Mines 49(6):187–194 (**in Chinese**)

Yang C, Liu SD, Wu RX (2017) Quantitative prediction of water volumes within a coal mine underlying limestone strata using geophysical methods. Mine Water Environ 36:51–58

Yin HY, Wei JC, Liliana L, Guo JB, Xie DL, Li ZL, Zhao P (2016) Numerical simulation of water flow from the coal seam floor in a deep longwall mine in China. Mine Water Environ 35:243–252

Zhang JC, Liu TQ (1990) On depth of fissured zone in seam floor resulted from coal extraction and its distribution characteristics. J China Coal Soc 15(2):46–55 (**in Chinese**)

Zhang WQ, Li B, Yuan JD (2016) Detection and evaluation of crack development near the fault zone under the influence of coal mining. Electron J Geotech Eng 21(22):6841–6850